



Influence of Impermeable Elevated Bottom on the Wave Scattering due to Multiple Porous Structures

V. Venkateswarlu and D. Karmakar

Department of Applied Mechanics and Hydraulics National Institute of Technology Karnataka, Surathkal, Mangalore – 575025, India

†Corresponding Author Email: dkarmakar@nitk.edu.in

(Received December 4, 2018; accepted May 14, 2019)

ABSTRACT

The significance of multiple porous structures with finite spacing upon elevated seabed in the presence and absence of the leeward wall is examined under oblique wave impinging. Fluid propagation is assumed over the impermeable elevated bottom, and the fluid realm is separated into open water and porous structure regions. Continuity of the dynamic pressure and mass fluxes at the interfaces of the porous structure and the open water regions are adopted. The resistance and reactance due to the presence of the porous structure are taken into account using the porous structure dispersion relation. The numerical model is developed based on the eigenfunction expansion method along with matched velocity potentials at the interfaces of open water and the porous block regions. The wave reflection and transmission characteristics, energy damping and wave force impact on the leeward wall is analysed. The significance of the porosity, structural width, angle of incidence, width between the two structures and water chamber length is studied considering multiple porous blocks with finite spacing under oblique wave impinging in the presence and absence of leeward wall. The numerical results obtained in the present study agrees well with the theoretical and experimental results available in the literature. The present study illustrates that, with the increase in the number of porous blocks and gap between the porous blocks, the resonating trend is observed in the wave transformation and the influence of the elevated step height is revealed for the wave trapping.

Keywords: Multiple porous structures; Energy damping; Impermeable elevated bottom; Eigenfunction expansion method; Wave transformation.

NOMENCLATURE

<p>b_N position of the porous block</p> <p>C_f dimensionless turbulent resistant coefficient</p> <p>d width of the porous structure</p> <p>f linearized friction factor</p> <p>g gravitational acceleration</p> <p>G impedance of the porous medium</p> <p>h_j water depth in each of the region</p> <p>i imaginary number</p> <p>j different regions</p> <p>k_{jn} wave number in x-direction</p> <p>K_P intrinsic permeability</p> <p>K_r wave reflection characteristics</p> <p>K_t wave transmission characteristics</p> <p>K_d wave energy dissipation</p> <p>K_f wave force on leeside wall</p> <p>l wave number in z-direction</p> <p>L distance between the structure and wall</p> <p>M number of evanescent wave modes</p> <p>N number of porous structures</p>	<p>q instantaneous Eulerian velocity vector</p> <p>R_{10} complex amplitude of reflected wave</p> <p>s inertial effect of porous medium</p> <p>t time</p> <p>T wave period</p> <p>$T_{(2N+1)0}$ complex amplitude of transmitted wave</p> <p>w width between the two porous structures</p> <p>γ_{jn} wave number in y-direction</p> <p>δ_{mn} Kronecker delta</p> <p>ε porosity of the structure</p> <p>ζ_j free surface wave elevation</p> <p>θ angle of incoming wave trains</p> <p>λ wave length</p> <p>ϕ velocity potential</p> <p>ρ density of water</p> <p>ν kinematic viscosity</p> <p>ω wave frequency</p>
---	---

1. INTRODUCTION

In the last few decades, the novel design and development of various types of breakwaters are performed by scientists and engineers for the protection of offshore facilities and safe harbourage of ships in the port regions from the wave trains. The conventional breakwaters are preferred most to prevent the tremendous wave motion, and their primary purpose is to decrease the wave reflection, wave transmission phenomena and to increase the energy damping (Twu and Chieu, 2000). The recent studies suggest that the vertical porous breakwaters are one of the solution to mitigate the mainlands and coastal facilities from the oblique waves (Karmakar and Guedes Soares, 2015). Vertical porous breakwaters of different configurations are widely used to dissipate the wave energy. Among the vertical breakwaters, vertical porous structures on rubble mound bottom and elevated seabed are widely developed to provide better shelter to the maritime facilities (Das and Bora, 2014). Most of the ports and harbours such as Gudong and Zhuangxi Sea Dike in Shengli Oil Field in the Republic of China (Zhao *et al.*, 2017) are constructed with the porous blocks to create a gentle wave action for better maritime transport.

A significant study has been reported on wave scattering phenomena due to different types of porous barriers, plates and breakwaters using analytical methods and laboratory experiments. Newman (1965a) performed wave propagation in the presence of two-dimensional obstacles and extended the study to analyse the wave motion over the infinite step for the analysis of gravity wave scattering (Newman, 1965b). Sollitt and Cross (1972) investigated the wave motion inside the porous structure by considering the medium resistance and reactance offered by the structure with a new complex dispersion relation. The wave reflection and transmission coefficient is analysed using the eigenfunction expansion method, and validated with the experimental results. Newman (1974) investigated the wave scattering due to two closely spaced obstacles and, the second barrier/obstacle is observed effectively reducing the wave transmission coefficient. Dalrymple *et al.* (1991) obtained simplified analytical equations for finding the long-wave reflection and transmission characteristics due to the presence of the porous block for different configurations such as a porous block of finite width, semi-infinite width and porous block backed by the wall. The comparative study is presented between the full solution, plane-wave, and long-wave approximation for the wave reflection and the study reported that the deviation in the wave reflection is evident for $\gamma_{10}h_1 \geq 1.5$ in the presence of evanescent waves. Afterwards, Huang and Chao (1992), extended the study and analysed the velocity distribution within the porous structure. Recently, Liu and Li (2013) proposed a new analytical approach neglecting the porous structure dispersion relation in the formulation and the outcomes of the study are validated with the previous predictions.

Madsen and White (1976) presented the wave

transformation due to the trapezoidal breakwater, and the study is extended by Hsu and Wu (1998) to investigate the trapezoidal porous structure protected with a seaward plate as an effective energy absorber. Rambabu and Mani (2005) conducted the numerical study on multiple trapezoidal breakwaters and reported that the high energy damping is achieved with the porous breakwater compared with the impermeable breakwater. Koley *et al.* (2015a) examined the trapezoidal breakwater considering perforated outer layer and rigid inner layer placed on the sloping seabed. The leeward wall on the sloping seabed and uniform seabed with porous breakwater are analysed using coupled eigenfunction-boundary element method. The outer permeable layer shows the significant impact in reducing the wave force impact on the rigid inner layer due to the increase in the energy damping by the outer permeable layer.

Various types of breakwaters are used to attenuate the unwanted wave oscillations. The increase in the life period of the seawall is achieved on reducing the wave force impact on the seawall by constructing the various types of porous absorbers. The investigation on the wave interaction with the permeable walls (porous block backed by the wall) are widely performed. Madsen (1983) reported the iteration method to describe the friction factor in the theoretical analysis of porous structure backed by the leeward wall. The effect of the porosity and friction factor is studied in detail in reducing the wave reflection coefficient for long-wave approximation. Later, many similar studies were performed for a porous block placed on the sloping seabed (Mallayachari and Sundar, 1994; Zhu, 2001) and elevated seabed (Das and Bora, 2014) with the leeward wall. An extensive study on the wave scattering due to the porous structure away from the leeward wall is addressed by Zhu and Chwang (2001), Koley *et al.* (2015b), Zhao *et al.* (2016). The studies reported that the porous breakwater could be a preferable solution for providing better shelter to the coastal facilities and the spacing between porous structure and the leeward wall has a substantial role in the incident wave trapping.

Further, the permeable vertical walls are constructed to prevent the free passage of oblique incident waves, Dalian Chemical Production Terminal, Republic of China (Huang *et al.*, 2011) and Dieppe, France (Belorgey *et al.*, 2003) opted the permeable walls to protect the mainlands from incoming waves. The double vertical walls with finite spacing are suggested by Das *et al.* (1997), Sahoo *et al.* (2000), Koraim *et al.* (2011) to achieve the better wave trapping. After that, Karmakar and Guedes Soares (2015) proposed multiple bottom standing barriers to attenuate the wave energy using the least-squares approximation. The study suggested that the bottom standing barriers are acceptable as breakwaters, and free clamped barriers performance is significant as compared with moored clamped barriers to attenuate the maximum wave energy. Behera and Ng (2018), Kaligatla *et al.* (2018) extended the study considering variation in the seabed characteristics in the wave reflected region. Very recently, Somervell *et al.* (2018) proposed a simplified empirical relation

to find the friction factor with known parameters like porosity, width and depth of the structure using the eigenfunction expansion method. The experimental tests are performed for specific cases and validated with the theoretical results.

Experimental studies on wave interaction with the submerged structure are well documented in the literature. [Dattatri et al. \(1978\)](#) indicated that the performance of the semi-trapezoidal breakwater (seaside slope with leeward vertical) is better than the structures of regular configurations to attenuate the high wave action. [Sulisz \(1985\)](#) focused on the multi-layered trapezoidal structure using theoretical and experimental approach. The comparative study shows that the results of the hydraulic tests coincide with the theoretical results in the case of transmission characteristics. But a little variation between both numerical and experimental study is observed in the case of wave reflection characteristics. Especially for high wave steepness, theoretical results overestimate the experimental results. [Losada et al. \(1995, 1996, 1997\)](#), [Twu and Chieu \(2000\)](#), [Ting et al. \(2004\)](#), [Reddy and Neelamani \(2006\)](#), [Wang et al. \(2006\)](#) investigated the breakwaters with a series of experimental tests considering various types of structural configurations. Thereafter, [Laju et al. \(2011\)](#) concentrated on the relevance of friction factor for finding wave scattering due to pile supported skirt breakwaters using eigenfunction expansion approach and the results obtained are compared with the experimental study. In general, finding the friction factor is cumbersome and the study presented the friction factor in terms of relative submergence of the skirt walls. Recently, [Neelamani et al. \(2017\)](#) documented the multiple slotted vertical barriers with the rigid leeward wall to replace the sloping breakwater in the random wave fields. The study suggests that the size of rubble mound breakwater can be reduced up to 50% along with the reduction in 21% of construction cost with three slotted walls having 40% porosity without affecting the energy damping.

A significant study has been performed for the wave interaction with porous blocks placed on uniform seabed but very limited study is found for the wave scattering due to multiple porous blocks with finite spacing over the impermeable elevated bottom. In practice, the porous blocks are constructed near and far away from the shore and it is very challenging to find uniform/flat seabed for marine engineers. The continental shelves, natural and artificial sand bars are in common regarded as an elevated impermeable bottom. In the current manuscript, an attempt is made to examine the multiple porous blocks with finite spacing over impermeable elevated bottom ([Karmakar et al. 2010](#)) under oblique wave impinging. The wave scattering by the single and double porous structures are examined using the analytical method and the results obtained from the present study are validated with the available experimental results ([Twu and Chieu, 2000](#)) and numerical results ([Mallayachari and Sundar, 1994](#)). In addition, the wave reflection, transmission coefficient, energy damping and wave forces on the leeward wall is analysed. The relevance of the

leeward wall in the presence of the multiple porous blocks over the elevated bottom is documented and the influence of porosity, structural width, width between the structures and water chamber width on the oblique wave propagation are presented.

2. MATHEMATICAL FORMULATION

The present study investigates the oblique wave train incident on the multiple porous blocks. The geometry of the porous structure consists of homogenous porosity ε finite thickness d and water chamber width L . The physical problem is analysed in the three-dimensional Cartesian coordinate system with horizontal x - z directions, and the y -axis is considered to be downward positive. The foundation is assumed to be horizontal impervious with zero velocity in the case of open water region and porous block region. The porous structure is assumed to occupy till free surface level, and the elevated impermeable seabed height is varied. The $2N$ porous structures with and without leeward wall located at $x = -b_j$ for $j = 1, 2, \dots, 2N$ are examined as in Figs. 1(a,b). In the schematic diagram (Figs. 1a-b), the black portion depth shows the impermeable elevated bottom and dotted portion depth h_j for $j = 2, 4, \dots, 2N$ represents the porous structure height. However, the difference between the open water depth and depth of the porous structure shows the elevated step height ($h_{j+1} - h_j$) in each of the regions. In the case of the open water region, the water depth is kept constant, but the porous structure is placed on the elevated bottom of different depths.

The fluid is assumed to be occupy the regions $\bigcup_{j=1}^{2N+1} I_j$ with $I_1 \equiv (-b_1 \langle x \langle \infty, 0 \langle y \langle h_1$ sea side open water region $I_j \equiv (-b_j \langle x \langle -b_{j-1}, 0 \langle y \langle h_j$, $j=2, 3, \dots, 2N$ and $I_{2N+1} \equiv (-\infty \langle x \langle -b_{2N}, 0 \langle y \langle h_{2N+1}$ lee side open water region with $z \in (-\infty, \infty)$ for all I_j .

The subscript $j=2, 3, \dots, 2N$ represents the finite open water and porous block regions. Further, $j = 1$ and $j = (2N+1)$ represents seaside and leeside open water regions in the absence of the leeward wall. The region, $I_{2N+1} \equiv (-b_{2N} - L \langle x \langle -b_{2N}, 0 \langle y \langle h_{2N+1}$ is the leeside confined region in the presence of the leeward wall. It is assumed that the monochromatic incident wave is propagating from positive x - direction with an θ angle and is considered to be impinging on the first porous structure at $x = -b_1$. The fluid is considered to be inviscid, incompressible, irrotational and the porous structure is assumed as isotropic and homogeneous.

There exists the velocity potential namely $\Phi_j(x, y, z, t)$ and the free surface deflection $\zeta_i(x, z, t)$ which can be presented as $\Phi_j(x, y, z, t) = Re \{ \phi_j(x, y) e^{ilz - i\omega t} \}$ and $\zeta_j(x, y, z, t) = Re \{ \eta_j(x) e^{ilz - i\omega t} \}$ for open water and porous structure regions. Re denotes the real part and l is the component of wave number along the z - direction.

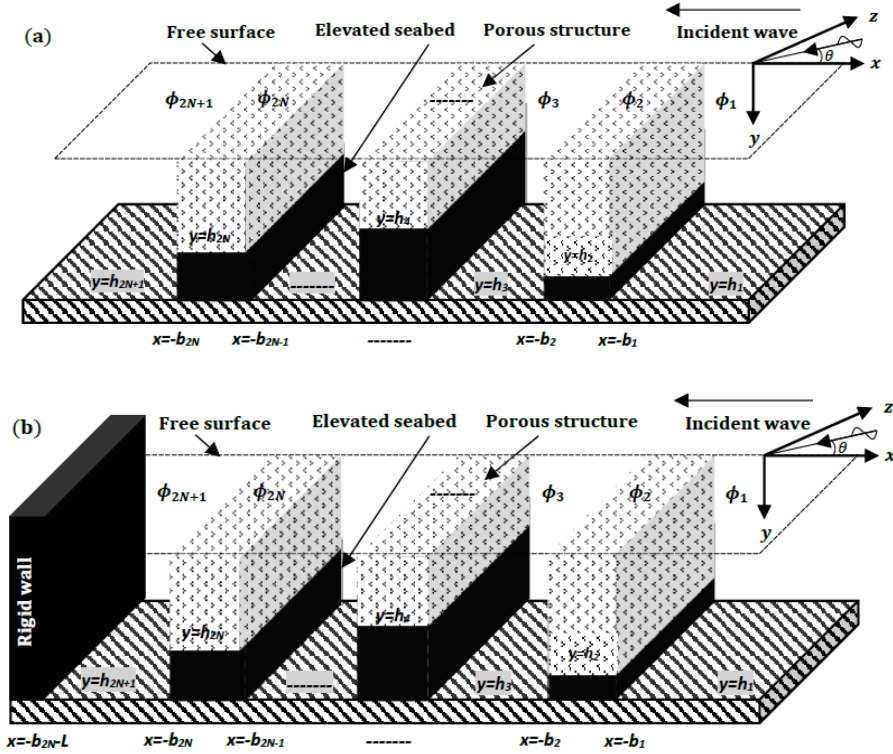


Fig. 1. Multiple porous structures on elevated bottom (a) without leeside wall and (b) with leeside wall.

The spatial velocity potential, $\phi_j(x, y)$ for $j=2,3,\dots,(2N+1)$ satisfies the partial differential equation given by

$$\left(\nabla_{xy}^2 - l^2\right)\phi_j(x, y) = 0 \quad \text{for } 0 < y < h_j. \quad (1)$$

where, $\nabla_{xy}^2 = \frac{\partial^2 \phi}{\partial x^2} + \frac{\partial^2 \phi}{\partial y^2}$ and $l = \gamma_{10} \sin \theta$ is the wave number in the z -direction. The linearized boundary condition in each of the regions I_j for $j=2,3,\dots,(2N+1)$ is of the form

$$\frac{\partial \phi_j(x, y)}{\partial y} - K_j \phi_j(x, y) = 0 \quad \text{at } y = 0, \quad (2)$$

where, $K_j = \omega^2/g$ for $j=1,3,\dots,(2N+1)$ in the case of open water region and $K_j = \omega^2(s - if)/g$ for $j=2,4,\dots,(2N)$ in the case of porous block region. The bottom boundary condition is given by

$$\frac{\partial \phi_j(x, y)}{\partial y} = 0 \quad \text{at } y = h_j, \quad j = 1, 2, \dots, (2N + 1). \quad (3a)$$

In the presence of the elevated seabed the velocity near the elevated step ($h_{j+1} - h_j$) for $j=1,3,\dots,(2N+1)$ is zero and is given by

$$\frac{\partial \phi_j(x, y)}{\partial x} = 0 \quad \text{at } x = b_j, \quad h_{j+1} < y < h_j \quad (3b)$$

In the general, the continuity of dynamic pressure

and velocity are applicable throughout the depth (Sollitt and Cross, 1972; Dalrymple *et al.*, 1991). On the other hand, in the case of elevated step porous structure, the continuity of pressure and velocity are applicable only for the porous structure depth h_i for $j=2,4,\dots,(2N)$ (Das and Bora, 2014) along with the zero-flow condition for the elevated step height. The continuity of dynamic pressure and mass flux (Karmakar *et al.*, 2010; Liu and Li, 2013; Das and Bora, 2014) at the interfaces along the horizontal x -direction is given by

$$\begin{aligned} \phi_j(x, y) &= G\phi_{(j+1)}(x, y), \\ \phi_{jx}(x, y) &= \varepsilon\phi_{(j+1)x}(x, y) \end{aligned} \quad (4a)$$

$$\text{at } x = -b_j, \quad j = 1, 3, \dots, (2N - 1), \quad 0 < y < h_{j+1},$$

$$\begin{aligned} G\phi_j(x, y) &= \phi_{(j+1)}(x, y), \\ \varepsilon\phi_j(x, y) &= \phi_{(j+1)x}(x, y) \end{aligned} \quad (4b)$$

$$\text{at } x = -b_j, \quad j = 2, 4, \dots, 2N, \quad 0 < y < h_j,$$

The no-flow condition near to the vertical rigid wall is given by

$$\frac{\partial \phi_j(x, y)}{\partial x} = 0 \quad \text{at } x = b_j + L, \quad j = (2N + 1). \quad (5)$$

where ε is the structural porosity, $G = s - if$ is the impedance of the porous medium, s is the medium reactance representing the inertial effect of the porous medium of the fluid flow (Chwang and Chan, 1998), i is imaginary number and f is the linearized friction factor. The friction factor and inertia effect of the porous medium (Sollitt and Cross, 1972;

(Dalrymple *et al.*, 1991) are computed using the relation given by

$$f = \frac{\frac{1}{V} \int_V dV \int_t^{t+T} \varepsilon^2 \left(\frac{\nu}{K_p} |q|^2 + \frac{C_f \varepsilon}{\sqrt{K_p}} |q|^3 \right) dt}{\int_V dV \int_t^{t+T} \varepsilon |q|^2 dt}, \quad (6a)$$

$$s = 1 + A_m \left[\frac{1 - \varepsilon}{\varepsilon} \right], \quad (6b)$$

where q is the instantaneous Eulerian velocity vector at any point, ν is the kinematic viscosity, K_p is the intrinsic permeability, V is the volume, C_f is dimensionless turbulent resistant coefficient, T is the wave period and A_m is the virtual added mass coefficient due to the wave impinging on the porous structure. The solution procedure and input values required for finding the friction factor is adopted from the previous works (Sollitt and Cross, 1972; Madsen, 1983; Das and Bora, 2014). In practice, the medium reactance/inertia is usually treated as unity due to the negligible added mass coefficient (Sollitt and Cross, 1972; Liu and Li, 2013) as the structure is in a fixed position. The far-field radiation condition is of the form

$$\phi_j(x) = \begin{cases} \left(I_{10} e^{-i\gamma_{10}x} + R_{10} e^{i\gamma_{10}x} \right) f_{10}(y) & \text{as } x \rightarrow \infty, \\ \left(T_{(2N+1)0} e^{i\gamma_{(2N+1)0}x} \right) f_{(2N+1)}(y) & \text{as } x \rightarrow -\infty, \end{cases} \quad (7)$$

with R_{10} and $T_{(2N+1)0}$ are the complex amplitudes of the reflected and transmitted waves. I_{10} is the incident wave potential, γ_{j0} for $j=1,3,\dots,(2N+1)$ are the positive real roots satisfies the open water dispersion relation given by

$$\omega^2 = g \gamma_{j0} \tanh \gamma_{j0} h_j. \quad (8a)$$

The roots γ_{j0} for $j = 2,4,\dots,2N$ satisfy the porous structure dispersion relation given by

$$\omega^2 (s - if) = g \gamma_{j0} \tanh \gamma_{j0} h_j. \quad (8b)$$

where, g is the gravitational acceleration γ_{j0} is wave number in open water and porous structure regions and ω is the wave frequency. Newton-Rapson method is employed to solve the open water region dispersion relation and perturbation method/step approach as in Mendez and Losada (2004) is applied to solve the porous structure dispersion relation.

3. METHOD OF SOLUTION

The present study is focused on the wave scattering due to the multiple porous structures upon elevated bottom in the absence and presence of the leeward wall.

3.1 Multiple Porous Blocks on the Elevated Seabed

The multiple porous blocks are designed to regulate the high wave action to create the

tranquillity in the bay regions. The gravity wave scattering due to the single and multiple porous blocks are investigated under oblique wave impinging. The fluid realm is separated into open water and porous structure regions and the velocity potentials in the open water and porous block regions are given by

$$\phi_1(x, y) = \left\{ I_{10} e^{-ik_{10}(x+b_1)} + R_{10} e^{ik_{10}(x+b_1)} \right\} f_{10}(y) + \sum_{n=1}^{\infty} \left\{ R_{1n} e^{-k_{1n}(x+b_1)} \right\} f_{1n}(y), \quad (9a)$$

for $-b_1 < x < \infty, 0 < y < h_1,$

$$\phi_j(x, y) = \sum_{n=0}^{\infty} \left\{ A_{jn} e^{-ik_{jn}(x+b_{j-1})} + B_{jn} e^{ik_{jn}(x+b_j)} \right\} f_{jn}(y)$$

for $-b_j < x < -b_{j-1}, 0 < y < h_j, j = 2,3,\dots,2N,$ (9b)

$$\phi_{2N+1}(x, y) = \left\{ T_{(2N+1)0} e^{-ik_{(2N+1)0}(x+b_{2N})} \right\} f_{(2N+1)0}(y) + \sum_{n=1}^{\infty} \left\{ T_{(2N+1)n} e^{k_{(2N+1)n}(x+b_{2N})} \right\} f_{(2N+1)n}(y),$$

for $-\infty < x < -b_{2N}, 0 < y < h_{(2N+1)},$ (9c)

where, R_{1n}, A_{jn}, B_{jn} and $T_{(2N+1)n}$ for $n=0,1,2,\dots$ and $j=1,2,3,\dots,2N$ are the unknown parameters to be determined, $d = -(b_{j+1}-b_j)$ for $j=1,2,3,\dots,2N$ is the thickness of the porous block and confined regions. The eigenfunctions in open water region and porous structure region is expressed in the form of $f_{jn}(y)$ for $j=1,2,3,\dots,(2N+1)$ are given by

$$f_{jn}(y) = \frac{\cosh \gamma_{jn} (h_j - y)}{\cosh \gamma_{jn} h_j} \quad \text{for } n=0,1,2,\dots \quad (10)$$

$\gamma_{jn} = i\gamma_{jn}$ for $n=1,2,3,\dots$, in the case of open water region and the eigenvalues γ_{jn} satisfy the open water and porous structure dispersion relations given by

$$\omega^2 = g \gamma_{jn} \tanh \gamma_{jn} h_j \quad \text{for } j = 1,3,\dots,(2N+1), n = 0, \quad (11a)$$

$$\omega^2 (s - if) = g \gamma_{jn} \tanh \gamma_{jn} h_j \quad \text{for } j = 2,4,\dots,2N, n = 0,1,2,\dots \quad (11b)$$

with $\gamma_{jn} = i\gamma_{jn}$ for $n=1,2,3,\dots$ and water depth $h_j = h_1$ for $j = 1,3,\dots,(2N+1)$ in the case of open water region. The dispersion relation has positive real root γ_{j0} with $\gamma_{jn}^2 = k_{jn}^2 + l^2, n=0$ where $l = \gamma_{10} \sin \theta$, θ is the angle of wave incidence k_{jn} is the component of wave number along x-direction and γ_{jn} is the wave number in the y-direction. In addition, there are purely imaginary roots γ_{jn} with $\gamma_{jn}^2 = k_{jn}^2 + l^2$ for $n = 1,2,3,\dots$. The eigenfunctions $f_{jn}(y)$ for $j=1,2,3,\dots,(2N+1)$ satisfies the orthogonality relation of the form

$$\langle f_{jm} f_{jm} \rangle_{j=1,3,\dots,(2N+1)} = \begin{cases} 0 & \text{for } m \neq n, \\ C'_n & \text{for } m = n, \end{cases}$$

and

$$\langle f_{jm} f_{jm} \rangle_{j=2,4,\dots,2N} = \begin{cases} 0 & \text{for } m \neq n, \\ C''_n & \text{for } m = n, \end{cases} \quad (12)$$

with respect to the orthogonal mode-coupling relation defined by

$$\langle f_{jm} f_{jn} \rangle_{j=1,3,\dots,(2N+1)} = \int_0^{h_j} f_{jm}(y) f_{jn}(y) dy, \quad (13a)$$

$$\langle f_{jm} f_{jn} \rangle_{j=2,4,\dots,2N} = \int_0^{h_j} f_{jm}(y) f_{jn}(y) dy, \quad (13b)$$

where

$$C'_n|_{j=1,3,\dots,(2N+1)} = \left\{ \frac{2\gamma_{jn} h_j + \sinh 2\gamma_{jn} h_j}{4\gamma_{jn} \cosh^2 \gamma_{jn} h_j} \right\} \text{ and}$$

$$C''_n|_{j=2,4,\dots,2N} = \left\{ \frac{2\gamma_{jn} h_j + \sinh 2\gamma_{jn} h_j}{4\gamma_{jn} \cosh^2 \gamma_{jn} h_j} \right\} \quad (14)$$

with $C'_n|_{j=1,3,\dots,(2N+1)}$ for $n=1,2,3,\dots$ are found by

substituting $\gamma_{jn} = i\gamma_{jn}$. In order to determine the unknown coefficients, the mode coupling relation (13a,b) is employed on the velocity potential $\phi_j(x,y)$ and $\phi_{jx}(x,y)$ with the eigenfunction $f_{jm}(y)$ along with continuity of dynamic pressure and mass fluxes as in Eqs. 4 (a, b) across the vertical interface $x = -b_j$, $0 < y < h_j$ for $j=1,3,\dots,(2N-1)$ to obtain

$$\langle \phi_j(x,y), f_{jm}(y) \rangle = \int_0^{h_j} \phi_j(x,y) f_{jm}(y) dy$$

$$= \left\{ \int_0^{h_{j+1}} + \int_{h_{j+1}}^{h_j} \right\} \phi_j(x,y) f_{jm}(y) dy$$

$$= G \int_0^{h_{j+1}} \phi_j(x,y) f_{jm}(y) dy + \int_{h_{j+1}}^{h_j} \phi_j(x,y) f_{jm}(y) dy$$

for $m = 0,1,2,\dots$ and $j = 1,3,\dots,(2N-1)$.

(15)

$$\langle \phi_{jx}(x,y), f_{jm}(y) \rangle = \int_0^{h_j} \phi_{jx}(x,y) f_{jm}(y) dy$$

$$= \varepsilon \left\{ \int_0^{h_{j+1}} + \int_{h_{j+1}}^{h_j} \right\} \phi_{(j+1)x}(x,y) f_{jm}(y) dy, \quad (16)$$

for $m = 0,1,2,\dots$ and $j = 1,3,\dots,(2N-1)$.

Again, the mode coupling relation (13a,b) is employed on the velocity potential $\phi_{j+1}(x,y)$ and $\phi_{(j+1)x}(x,y)$ with the eigenfunction $f_{(j+1)m}(y)$ along continuity of dynamic pressure and mass fluxes as in Eqs. (4a, b) across the vertical interface $x = -b_j$, $0 < y < h_j$ to obtain

$$\langle \phi_{j+1}(x,y), f_{(j+1)m}(y) \rangle = \int_0^{h_{j+1}} \phi_{j+1}(x,y) f_{(j+1)m}(y) dy$$

$$= \left\{ \int_0^{h_j} + \int_{h_j}^{h_{j+1}} \right\} \phi_{j+1}(x,y) f_{(j+1)m}(y) dy$$

$$= G \int_0^{h_j} \phi_j(x,y) f_{(j+1)m}(y) dy$$

$$+ \int_{h_j}^{h_{j+1}} \phi_{j+1}(x,y) f_{(j+1)m}(y) dy,$$

for $m = 0,1,2,\dots$ and $j = 2,4,\dots,2N$.

(17)

$$\langle \phi_{(j+1)x}(x,y), f_{(j+1)m}(y) \rangle$$

$$= \int_0^{h_{j+1}} \phi_{(j+1)x}(x,y) f_{(j+1)m}(y) dy$$

(18)

$$= \varepsilon \left\{ \int_0^{h_j} + \int_{h_j}^{h_{j+1}} \right\} \phi_{jx}(x,y) f_{(j+1)m}(y) dy,$$

for $m = 0,1,2,\dots$ and $j = 2,4,\dots,2N$.

It may be noted that the zero-horizontal velocity at $x = -b_j$, is applied for $h_{j+1} < y < h_j$, $j=1,3,\dots,(2N-1)$ and $h_j < y < h_{j+1}$, $j=2,4,\dots,(2N)$ as in Eq. (3b) to obtain

$$\int_{h_j}^{h_{j+1}} \phi_{(j+1)x}(x,y) f_{jm}(y) dy = 0,$$

for $m = 0,1,2,\dots$ and $j = 1,3,\dots,(2N-1)$.

(19a)

$$\int_{h_j}^{h_{j+1}} \phi_{jx}(x,y) f_{(j+1)m}(y) dy = 0,$$

for $m = 0,1,2,\dots$ and $j = 2,4,\dots,2N$.

(19b)

The infinite series sums shown in the algebraic Eqs. (15), (16), (17) and (18) are truncated upto finite M terms and a linear system of for $4_j (M+1)$ for $j=2,4,\dots,(2N)$ algebraic equations is obtained to solve the $4_j (M+1)$ unknown coefficients. The wave reflection and transmission characteristics due to the porous structure on the elevated seabed is given by

$$K_r = \left| \frac{R_{10}}{I_{10}} \right| \quad \text{and} \quad K_t = \left| \frac{T_{(2N+1)0}}{I_{10}} \right| \quad (20a)$$

The wave energy damping due to the presence of the porous block is investigated based on the relation as in [Chwang and Chan \(1998\)](#) given by

$$K_d = 1 - K_r^2 - K_t^2. \quad (20b)$$

3.2 Multiple Porous Blocks on the Elevated Seabed with Leeward Wall

The significance of the multiple porous structures over elevated seabed away from the leeward wall is studied to understand the wave transformation

mechanism. The velocity potentials in open water and porous structure regions are similar as in Eqs. (9a, b) and the leeward region velocity potential is obtained as

$$\phi_1(x, y) = \left\{ I_{10} e^{-ik_{10}(x+b_1)} + R_{10} e^{ik_{10}(x+b_1)} \right\} f_{10}(y) + \sum_{n=1}^{\infty} \left\{ R_{1n} e^{-k_{1n}(x+b_1)} \right\} f_{1n}(y), \quad (21a)$$

for $-b_1 < x < \infty, 0 < y < h_1$,

$$\phi_j(x, y) = \sum_{n=1}^{\infty} \left\{ A_{jn} e^{-ik_{jn}(x+b_{j-1})} + B_{jn} R_{10} e^{ik_{jn}(x+b_j)} \right\} f_{jn}(y)$$

for $-b_j < x < -b_{j-1}, 0 < y < h_j, j = 2, 3, \dots, 2N$,

(21b)

$$\phi_{2N+1}(x, y) = \left\{ T_{(2N+1)0} e^{-ik_{(2N+1)0}(x+b_{2N})} + D_{(2N+1)0} e^{ik_{(2N+1)0}(x+b_{2N}+L)} \right\} f_{(2N+1)0}(y) + \sum_{n=1}^{\infty} \left\{ T_{(2N+1)n} e^{k_{(2N+1)n}(x+b_{2N})} + D_{(2N+1)n} e^{-k_{(2N+1)n}(x+b_{2N}+L)} \right\} f_{(2N+1)n}(y)$$

for $-(b_{2N} + L) < x < -b_{2N}, 0 < y < h_{2N+1}$.

(21c)

Further Eq. (21c) is simplified using the no-flow condition near to the leeside wall as in Eq. (5) given by

$$\phi_{2N+1}(x, y) = T_{(2N+1)0} \left\{ \begin{matrix} e^{-ik_{(2N+1)0}(x+b_{2N})} \\ + e^{ik_{(2N+1)0}(x+b_{2N}+L)} \end{matrix} \right\} f_{(2N+1)0}(y) + \sum_{n=1}^{\infty} T_{(2N+1)n} \left\{ \begin{matrix} e^{k_{(2N+1)n}(x+b_{2N})} \\ + e^{-k_{(2N+1)n}(x+b_{2N}+L)} \end{matrix} \right\} f_{(2N+1)n}(y)$$

for $-(b_{2N} + L) < x < -b_{2N}, 0 < y < h_{2N+1}$.

(21d)

The matching conditions as in Eqs. (4a, b) and mode coupling relation as in Eqs. (13a, b) is applied to obtain system of linear equations as in section 3.1. The infinite series sums are truncated upto finite M terms and a linear system of $4_j (M + 1)$ for $j=2, 4, \dots, (2N)$ algebraic equation is obtained to solve the $4_j (M + 1)$ unknown coefficients. The wave force acting on the leeside wall K_f is given by

$$K_f = \frac{F_w}{2\rho gh_1 I_0} \quad (22a)$$

with

$$F_w = i\rho\omega \int_0^{h_j} \phi_{(2j+1)}(x, y) dy \text{ at } x = -\left\{ (b_{2j} - b_1) + L \right\}$$

for $j = 1, 2, \dots, 2N$ (22b)

where I_0 is the amplitude of the incident wave potential considered to be unity.

4. RESULTS AND DISCUSSIONS

The present study elaborates the wave reflection K_r , transmission K_t , energy dissipation K_d , and wave force impact on leeside wall K_f due to multiple porous blocks with finite spacing placed over the elevated bottom in the presence and absence of the leeward wall. The influence of the evanescent waves on the wave transformation due to the single porous block kept on elevated seabed is investigated and presented in Table 1. It is observed that, the variation in the K_r and K_t with the increase in the evanescent waves converges for $M > 20$. So in the present study evanescent modes are truncated for $M = 30$ to perform the hydrodynamic analysis of porous structure placed over elevated step.

Table 1 Convergence study with increase in the evanescent waves for $f = 0.5, d/h_1 = 1.25, \epsilon = 0.4, \gamma_{10}h_1 = 0.5$ and 10% elevated step height

Wave reflection coefficient (K_r)				
M	$\theta = 0^\circ$	$\theta = 15^\circ$	$\theta = 30^\circ$	$\theta = 45^\circ$
0	0.4875	0.4742	0.4323	0.3550
10	0.4714	0.4581	0.4163	0.3396
20	0.4780	0.4649	0.4235	0.3476
30	0.4793	0.4662	0.4253	0.3495
40	0.4793	0.4662	0.4253	0.3495
Wave transmission coefficient (K_t)				
M	$\theta = 0^\circ$	$\theta = 15^\circ$	$\theta = 30^\circ$	$\theta = 45^\circ$
0	0.6559	0.6610	0.6768	0.7039
10	0.6740	0.6788	0.6936	0.7188
20	0.6786	0.6836	0.6991	0.7256
30	0.6771	0.6820	0.6973	0.7242
40	0.6771	0.6820	0.6973	0.7242

In order to verify the present model outcomes, the wave transformation due to the single and double porous blocks is analysed and study outcomes are validated with the numerical and hydraulic tests results available in the literature. [Mallayachari and Sundar \(1994\)](#) reported the wave reflection phenomenon due to the permeable breakwater with leeward wall using the numerical model based on green's identity formula. The present study examine the structural configuration as in [Mallayachari and Sundar \(1994\)](#) using the matched eigenfunction expansions. In Fig. 2(a) the wave reflection K_r due to the permeable structure backed by rear wall is presented with variation in the structural width for various porosities within $0.2 < \epsilon < 0.8$. It is noted that, the increase in the structural porosity shows the significant decrease in the K_r due to increase in the wave damping. The minimum wave reflection is obtained at $\gamma_{10}h_1 = 1.5$ for the porosities within $0.2 < \epsilon < 0.8$ may be due to formation of the standing waves. However, the increase in $\gamma_{10}d$ shows the uniform results in the K_r within $3 < \gamma_{10}d < 8$ for different porosities. In addition, the correlation between the present study and [Mallayachari and Sundar \(1994\)](#) is quite acceptable in the wave reflection K_r as shown in Fig. 2(a). On the other hand, the energy damping K_d due to the double porous blocks placed on uniform rigid seabed is analysed with variation in the dimensionless wavelength h_1/λ using matched eigenfunction expansions and validated with the experimental results presented by

Twu and Chieu (2000). Almost 90% of energy damping K_d is achieved (Fig. 2b) due to the double porous structure and the correlation between the experimental and analytical results in the K_d is observed considerable.

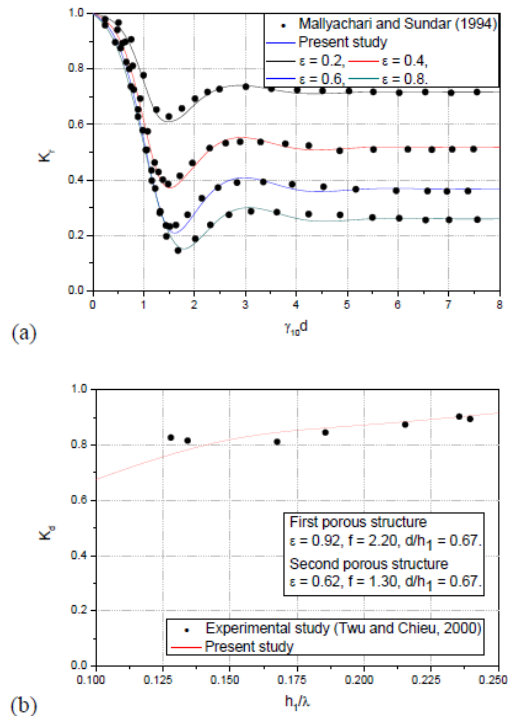


Fig. 2. Comparative study of (a) K_r versus $\gamma_{10}d$ for the porous block backed by wall (Mallyachari and Sundar, 1994) and (b) K_d versus h_1/λ for double porous structure (Twu and Chieu, 2000) on uniform seabed.

The numerical outcomes obtained from the present approach converge well with the analytical (Fig. 2a) and experimental predictions (Fig. 2b) available in the literature, and the study is extended to analyse the hydrodynamic performance of multiple porous blocks placed on elevated impermeable bottom in the presence and absence of leeward wall using the eigenfunction expansion technique.

4.1 Multiple Porous Blocks on the Elevated Bottom

The significance of multiple porous blocks with finite spacing over the elevated bottom is examined in the present section. The wave transformation due to the change in elevated step height, structural porosity, structural thickness d , width between the two porous structures w and angle of incidence θ are investigated in detail.

4.1.1 Single Porous Block Placed on Elevated Bottom

The impact of the elevated step height on the wave transformation due to presence of porous block is analysed. In Figs. 3(a,b), the K_r and K_t versus $\gamma_{10}d$ is plotted for various values of elevated step height h_2/h_1 for a single porous structure and the elevated step height is varied within $0.75 \leq h_2/h_1 \leq 1.0$.

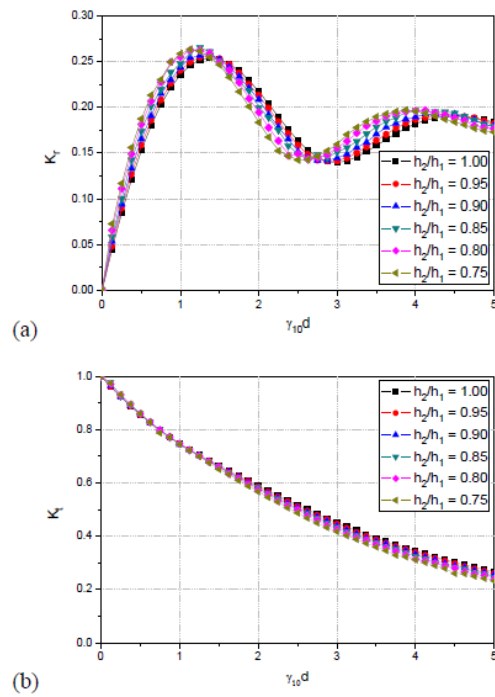


Fig. 3. Variation in (a) K_r and (b) K_t versus $\gamma_{10}d$ for different elevated step height with $\epsilon = 0.8, \gamma_{10}d=0.5, f=0.5, \theta = 0^\circ$.

The variation in the K_r (Fig. 3a) is significant with variation in the elevated step height. The resonating pattern is obtained in the K_r with increase in the $\gamma_{10}d$ for $0.75 \leq h_2/h_1 \leq 1.0$. The K_r is observed to converge due to the change in h_2/h_1 at particular intervals ($\gamma_{10}d = 1.5, 2.75$ and 4.5). The periodic increase and decrease in the K_r is obtained as compared with flat seabed due to increase in h_2/h_1 . Minor variation is observed in the transmission characteristics (Fig. 3b) between the uniform bottom and elevated bottom. The increase in the step height shows the small variation in the K_t due to the increase in K_r within $2 < \gamma_{10}d < 5$.

However, the increase in the elevated step height shows little increase in the wave reflection at each of the resonating peak and little decrease in the wave transmission coefficient, which may be due to the change in the energy damping by the porous structure.

4.1.2 Double Porous Blocks Placed on Elevated Bottom

In Fig. 4, the impact of the elevated step height on the K_r is studied for double porous structures. The increase in the elevated step height shows the increase in the K_r within $0^\circ \leq \theta \leq 60^\circ$ compared with flat bottom and it is obvious in the wave structure interaction problems. The optimum aim of the elevated step porous block is to increase the wave energy damping, but it is found that 51% increase in the K_r is noted with 25% increase in the elevated step height at $\theta = 0^\circ$ as in Fig. 4. In order to increase the performance of the structure in the energy damping, the present study suggests the elevated step height within $0.85 \leq h_2/h_1 \leq 0.9$, which is beneficial to

construct the porous structures upon the artificial elevated seabed without affecting the energy dissipation.

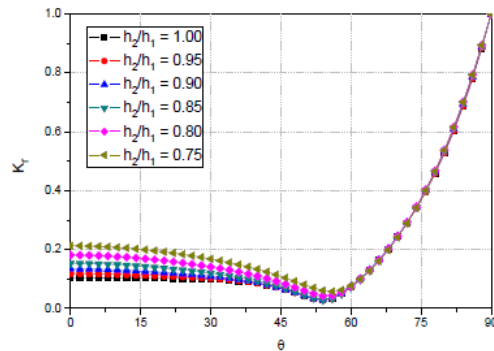


Fig. 4. Variation in the K_r versus θ for different elevated step height with $\varepsilon = 0.8$, $w / h_1 = 1$, $\gamma_{10}d = 0.5$, $f = 0.5$ and $d / h_1 = 4$.

The structural porosity plays an immense role in the wave transformation. In general, minimum porosity yields low energy dissipation and maximum porosity shows high energy dissipation. However, the stability of the structure which depends upon the self-weight of the breakwater also influences the wave transformation. In most of the conditions the porosity is considered within $0.4 < \varepsilon < 0.8$ (Sollitt and Cross, 1972; Madsen, 1983; Mallayachari and Sundar, 1994). In Figs. 5(a-c), the impact of the structural porosity within $0.4 < \varepsilon < 0.8$ is studied on the wave scattering in the presence of two porous blocks. The resonating trend is observed in the reflection characteristics K_r (Fig. 5a) which may be due to wave trapping by the confined region existing between the two porous structures. The sudden variation in the wave reflection coefficient is noticed within $0.1 \leq \gamma_{10}d \leq 3.5$ and the resonating pattern decreases with the increase in the porosity. Around 28% and 57% decrease in the K_r is noted for $\varepsilon = 0.6$ and $\varepsilon = 0.8$ as compared with $\varepsilon = 0.4$ at $\gamma_{10}d = 2.25$. However, the drastic variation in the K_r is only due to increase in the K_t and K_d . In Fig. 5(b), the increase in the ε shows the increase in the K_t due to the high permeability of the structure, which causes the high interaction between the fluid and structure and results in high energy absorption. The increase in the structural porosity shows the significant increase in the K_t within $0.1 \leq \gamma_{10}d \leq 3.5$, thereafter, the K_t reaches to the minimum values. Hence, the increase in the structural porosity shows the significant increase in the K_t for specific range and enhances the energy damping.

In the case of wave energy damping (Fig. 5c), it is noticed that the resonating trend disappears with the increase in porosity and maximum energy damping of $K_d > 80\%$ is achieved for structural porosity $\varepsilon = 0.8$ within $3.25 \leq \gamma_{10}d \leq 5.0$. Almost 15% difference is observed in the K_d for $0.4 < \varepsilon < 0.8$. However, the increase in the porosity ε shows the preferable increase in K_d , which may be due to the wave trapping in the finite spacing.

The structural width is an essential phenomenon in

the wave blocking, especially the waves of higher wavelength can be attenuated for significant structural width. The present condition elaborates the effect of the non-dimensional structural width d / h_1 on wave scattering for a double porous block kept on elevated bottom. In Figs. 6(a,b), the K_r , K_t versus angle of incidence θ is presented with variation in the d / h_1 for $\varepsilon = 0.4$ (Fig. 6a) and $\varepsilon = 0.8$ (Fig. 6b).

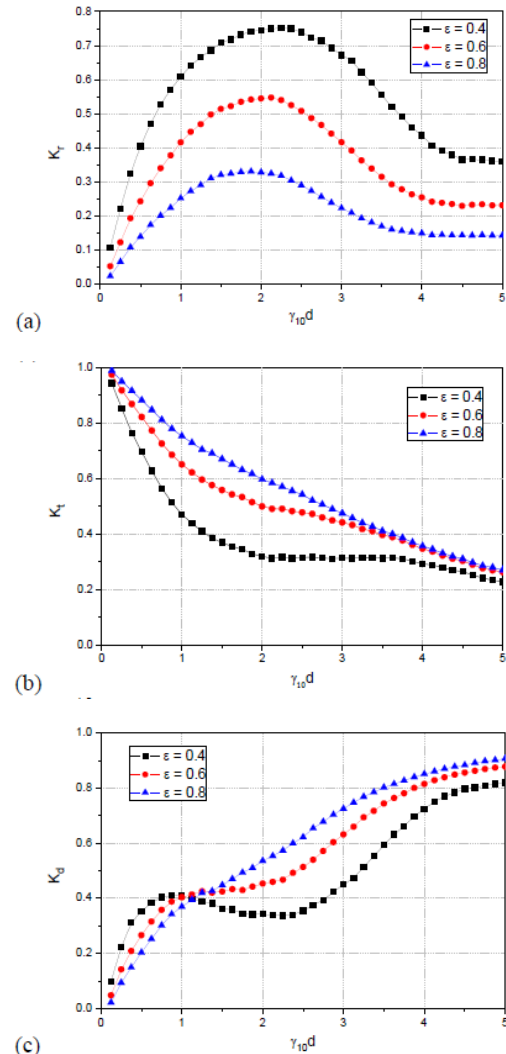


Fig. 5. Variation in (a) K_r (b) K_t and (c) K_d versus $\gamma_{10}d$ for different porosities with $\gamma_{10}d h_1 = 0.5$, $w / h_1 = 5$, $h_2 / h_1 = 0.9$, $d_1 = d_2 = d / 2$, $f = 0.5$ and $\theta = 0^\circ$.

The increase in the d / h_1 shows an increase in the K_r and minimum K_r from the structure is observed at $\theta = 74^\circ$ (Fig. 6a) and $\theta = 54^\circ$ (Fig. 6b) for all nondimensional structural width within $0.25 < d / h_1 < 2$. The minimum K_r at $\theta = 74^\circ$ (Fig. 6a) and $\theta = 54^\circ$ (Fig. 6b) is due to the formation of standing waves at that particular angle of incidence which may be termed as critical angle. However, increase in the d / h_1 illustrates significant reduction in the K_t for $\varepsilon = 0.4$ (Fig. 6a) and $\varepsilon = 0.8$ (Fig. 6b). It may be noted that for $d / h_1 = 2$ the variation in K_r and K_t is more as compared to other non-dimensional width of the

structure. High wave reflection is observed for all structural width d/h_1 at $\varepsilon = 0.4$ as compared with $\varepsilon = 0.8$ but the transmission coefficient is almost similar for $\varepsilon = 0.4$ and $\varepsilon = 0.8$. This shows that the increase in the ε presents a preferable decrease in the wave reflection characteristics and less variation in transmission coefficient is noted between $\varepsilon = 0.4$ and $\varepsilon = 0.8$ due to the increase in the energy damping by fluid and porous structure interaction. However, the minimum K_t can be achieved with increase in the structural width.

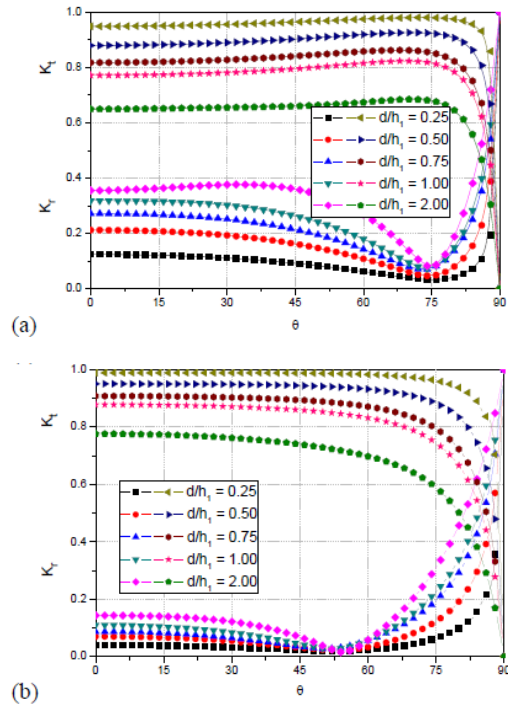


Fig. 6. Variation in K_r and K_t versus θ for different values of d/h_1 for $\gamma_{10d} h_1 = 0.5, h_2/h_1 = 0.9, w/h_1 = 1, f = 0.5, d_1 = d_2 = d/2$, (a) $\varepsilon = 0.4$ and (b) $\varepsilon = 0.8$.

4.1.3 Triple Porous Blocks Placed on Elevated Bottom

In the case of triple porous structures, one of the influencing parameters in wave blocking is finite spacing between the two successive porous structures w/h_1 . The variation in the wave transformation is presented with variation in the w/h_1 and the resonating trend in the wave scattering is clearly seen. The resonating peaks in the K_r (Fig. 7) and resonating minor troughs in the K_t (Fig. 7) is obtained with the increase in the w/h_1 and secondary resonating peaks in between the resonating high peaks is also noticed. This indicates that, there is either increase or decrease in the K_r and K_t due to wave trapping by finite spacing w/h_1 . In practice, the resonating peaks and troughs suggests that, the optimum dimensionless width between the two structures can be achieved in the design and construction of the multiple breakwaters for better wave trapping in the confined region. Thus, the optimum w/h_1 for $\gamma_{10d} h_1 = 0.5$ is observed to be

$(j\pi) < w/h_1 < (j+1)\pi$ for $j = 0, 1, 2, \dots$ in the presence of triple structure placed on elevated seabed with finite spacing as in Fig. 7.

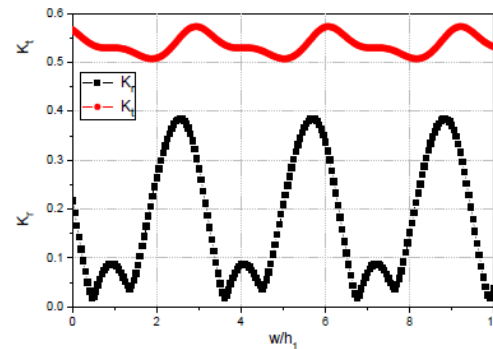


Fig. 7. Variation in K_r and K_t versus w/h_1 for $d_1/h_1 = 1, d_2/h_1 = 1, d_3/h_1 = 1, h_2/h_1 = 0.9, f = 0.5, \varepsilon = 0.4$ and (b) $\varepsilon = 0.8, \gamma_{10d} h_1 = 0.5$ and $\theta = 0^\circ$.

4.1.4 Comparative Study of Multiple Porous Blocks

In order to study the relevance of the multiple porous blocks in the wave blocking, a comparative study is performed by increase in the number of porous structures for the case of plane-wave approximation. The numerical parameters such as friction factor $f = 2$ width between any two porous structures $w/h_1 = 1$ porosity of the each structure $\varepsilon = 0.4$ and the elevated step height $h_2/h_1 = 0.8$ are kept fixed for the comparative study. The width of the single porous block is separated into equal multiple porous blocks. In Figs. 8(a,b) the K_r (Fig. 8a) and the K_t (Fig. 8b) is plotted versus γ_{10d} with increase in the number of structures

The variation between the single, double and triple porous structures in the K_r is evident in the design of coastal structures. The performance of the four and five structures shows almost similar estimation in the K_r . It is noticed that the increase in the number of porous blocks N shows the decrease in the K_r within $0.1 < \gamma_{10d} < 2.5$ which may be due to the wave trapping by multiple confined regions existing between the multiple structures. Afterwards, the increase in the N shows the almost similar estimation in the K_r within $2.5 < \gamma_{10d} < 5$. On the other hand, the relevance of the multiple porous structures placed on elevated seabed with multiple confined regions w/h_1 in the reduction of transmission coefficient in Fig. 8(b) is studied. It is noted that the increase in the N shows the little decrease in the K_t within $0.1 < \gamma_{10d} < 1.5$. Afterwards, the K_t reaches to zero due to the wave blocking by multiple porous blocks. The variation in the K_t is mainly due to the increase in the multiple confined regions w/h_1 which causes more energy damping as compared with the single structure.

4.2 Multiple Porous Blocks Placed on the Elevated Bottom with Leeward Wall

The seawalls are one of the common structures constructed in many locations for the protection of the main lands. In the present section the necessity of

the single and multiple porous structures placed on elevated seabed with the water chamber length L/h_1 and leeside wall is analysed for the protection of main lands from high wave action.

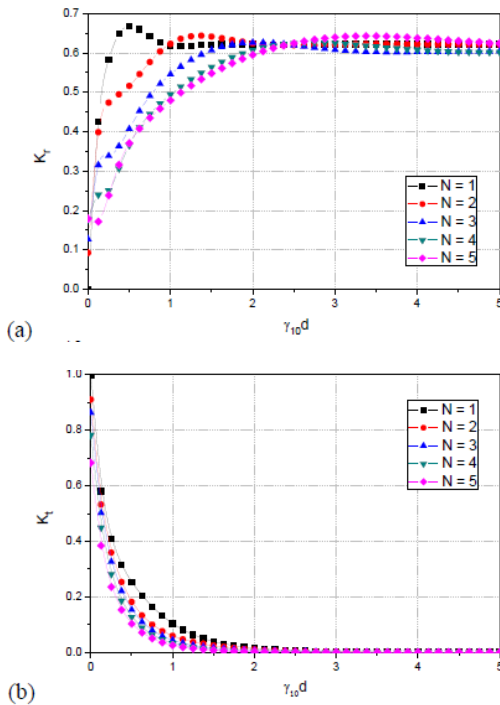


Fig. 8. Comparative study between the multiple structures in (a) K_r and (b) K_f versus $\gamma_{10}d$ with $\varepsilon = 0.4, f = 2, \gamma_{10}h_1 = 0.5, \theta = 0^\circ, w/h_1 = 1$ and $h_2/h_1 = 0.8$.

4.2.1 Single Porous Block Placed on Elevated Bottom with Leeward Wall

The impact of dimensionless thickness of the elevated step porous structure on the wave transformation phenomenon is examined. The wave reflection coefficient K_r (Fig. 9a) and wave force impact on leeside wall K_f (Figs. 9b) due to the single porous block with the leeward wall are studied varying angle of incidence θ for the different structural widths within $0.25 \leq d/h_1 \leq 2$.

It is found that, the increase in d/h_1 shows the decrease in the K_r (Fig. 9a) due to the presence of the porous block with leeward wall and the critical angle moves towards the minimum angle of incidence for higher d/h_1 . The variation is clearly seen between $d/h_1 = 2$ and other combinations of width of the structure and it is significant in the design and construction of offshore structures. On the other hand, the K_f is calculated for various combinations of structural width (Fig. 9b) and the resonating trend is observed decreasing for higher values of d/h_1 and the minimum K_f is achieved for $d/h_1 = 2$. However, the decreasing trend in the K_r and K_f is noticed for higher values of d/h_1 due to the enhance in the energy damping by the porous block. This suggests that, the width of the structure $d/h_1 = 2$ is suitable in reducing the K_r and K_f in the presence of the leeward wall.

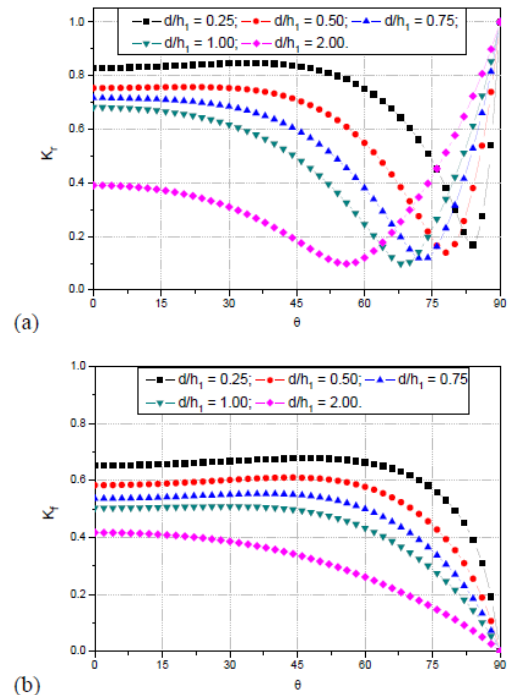


Fig. 9. Variation in (a) K_r and (b) K_f versus θ for different values of d/h_1 with $\gamma_{10}d/h_1 = 0.5, \varepsilon = 0.8, f = 0.5, L/h_1 = 1$ and $h_2/h_1 = 0.9$.

4.2.2 Double Porous Blocks Placed on Elevated Bottom with Leeward Wall

The wave reflection K_r and force impact on wall K_f for double porous structure with confined region is analysed in Figs. 10(a,b). The periodic increase and decrease in the K_r and K_f is noted and it is observed that there is an opposite trend existing between the K_r and K_f for variation in the L/h_1 .

The resonating peaks in the K_r and the resonating troughs in the K_f is observed at the same intervals and also the resonating troughs in the K_r , the resonating peaks in the K_f is observed due to the constructive and destructive interference of the monochromatic incident wave and the reflected waves. The present case suggests that, the L/h_1 is an influencing factor in order to design the porous blocks for better performance and it is noted that the porosity of the structure doesn't affect the periodic peaks in the K_f .

On the other hand, the wave scattering due to two porous structures (Figs. 11a,b) on elevated seabed with leeside wall is examined for different width of the structures. Fig. 11(a) shows the uniform values in K_r within $0^\circ < \theta < 60^\circ$ and further sharp decrease in the K_r within $60^\circ < \theta < 86^\circ$ is obtained for the nondimensional structural width considering $d/h_1 = 0.25$. Afterwards, the increase in the normalised structural width shows the resonating trend along with decrease in the K_r due to multiple confined regions. In Fig. 11(b), the wave force impact on the leeward wall K_f versus θ for different d/h_1 is plotted. The increase in the d/h_1 shows the decrease in the K_f and minimum K_f is observed for $d/h_1 = 2$.

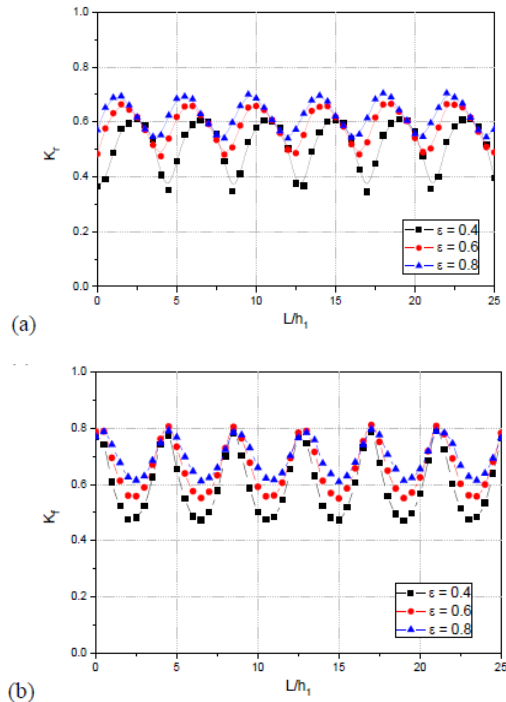


Fig. 10. Variation in (a) K_r and (b) K_f versus L/h_1 for different values of ε with $\gamma_{10}d/h_1 = 0.75$, $w/h_1 = 1$, $d/h_1 = 1$, $h_2/h_1 = 0.9$, $f = 0.5$, and $\theta = 0^\circ$.

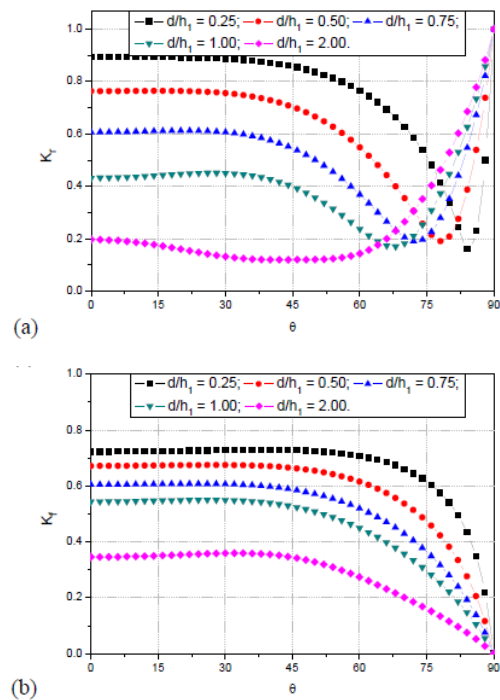


Fig. 11. Variation in (a) K_r and (b) K_f versus θ for different values of d/h_1 with $\gamma_{10}h_1 = 1$, $\varepsilon = 0.8$, $f = 0.5$, $w/h_1 = 1$, $L/h_1 = 1$ and $h_2/h_1 = 0.9$.

Around 7%, 16%, 24% and 51% reduction in the wave force K_f is achieved considering $0.5 < d/h_1 < 2$ as compared with the $d/h_1 = 0.25$ at $\theta = 0^\circ$. It is also noted that the 50% reduction in the K_r and 15% reduction in the K_f is obtained in the case of double porous structure (Figs. 11a,b) as compared with the

single porous structure (Figs. 9a,b) for $d/h_1 = 2$ at $\theta = 0^\circ$ due to the wave trapping by confined region existing between the two porous structures away from the rigid wall for a fixed width of the structure.

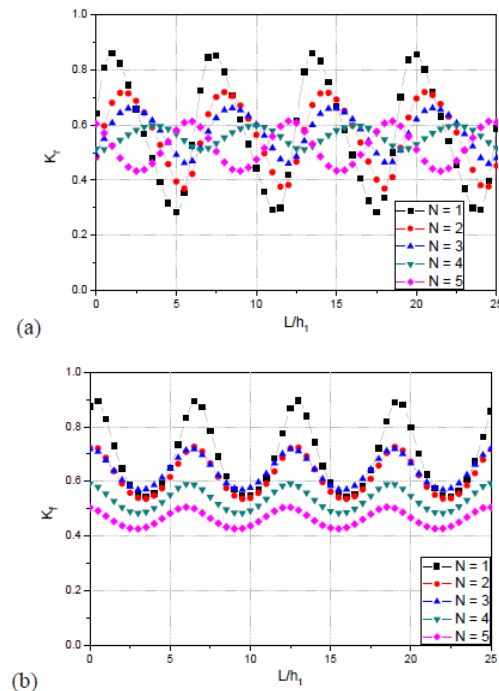


Fig. 12. Comparative study between the multiple structures in (a) K_r and (b) K_f versus L/h_1 with $\gamma_{10}h_1 = 0.5$, $\varepsilon = 0.4$, $f = 0.5$, $\theta = 0^\circ$, $d/h_1 = 2$, $w/h_1 = 1$ and $h_2/h_1 = 0.9$.

4.2.3 Comparative Study of Multiple Porous Blocks with Leaside Wall

In order to study the significance of the multiple porous structure with leaside wall in the wave blocking, a comparative study is performed by increase in the number porous structures under the assumption of plane-wave approximation. The numerical parameters $\gamma_{10}h_1 = 0.5$, $\varepsilon = 0.4$, $f = 0.5$, $\theta = 0^\circ$, $w/h_1 = 1$ and $h_2/h_1 = 0.8$ are kept fixed. The width of a single porous structure is considered to be $d/h_1 = 2$. Afterwards, the d/h_1 is separated into equal multiple structures for the purpose of comparison. Figs. 12(a,b) shows the variation in the K_r (Fig. 12a) and K_f (Fig. 12b) due to single and multiple structures with variation in the water chamber length L/h_1 . The resonating peaks are clear in the case of single porous block as compared with the multiple porous blocks and the resonating peaks and troughs in the K_r (Fig. 12a) is observed decreasing for higher number of porous blocks lying on elevated bottom which may be due to the increase in the confined regions w/h_1 and the transmitted wave from the first porous block reflected back by the subsequent porous block and interacting with incoming waves. Similarly, the K_f (Fig. 12b) is noted decreasing with the increase in the multiple structures and the resonating peaks and troughs are observed to be high for $N = 1$ and these resonating peaks and troughs decreases with the increase in the multiple porous

blocks. The increase in the confined regions is the major reason behind the decrease in the K_f . The present study suggests that the multiple structures are the better solution in the wave blocking and the resonating peaks and troughs on the wave reflection K_r and wave force in the leeside wall K_f can be reduced considering multiple porous blocks. The resonating troughs are observed in the K_f at particular intervals. These resonating troughs also encourages the formation of clapotis nodes (Twu and Lin, 1991). These clapotis nodes are helpful in the design of coastal structures to find the optimum water chamber length for the construction of the porous structure away from the leeward wall to achieve better wave trapping in practice.

5. CONCLUSION

The oblique wave scattering due to the single and multiple porous blocks are examined using the matched eigenfunction expansion method. The following conclusions are drawn, and the outcomes are summarised below:

- The numerical results in the present study are validated with the previous theoretical studies performed by notable authors.
- The 90% energy damping in the presence of two porous structures is observed, and the numerical results are validated with the experimental result available in the literature.
- The effect of elevated step height on wave scattering is examined and 10% - 15% elevated step height with porous structure is suggested to enhance the energy damping.
- The minimum structural porosity shows the high reflection, low transmission, energy dissipation and wave force on the leeside wall.
- In the case of triple porous structure, the optimum width between the two structures w/h_1 for $\gamma_{10}h_1=0.5$ is observed to satisfy the relation $(j\pi) < w/h_1 < (j+1)\pi$ for $j=0,1,2,3,\dots$, to achieve the minimum wave reflection and transmission coefficients.
- In the case of porous block with leeside wall the porosity within $0.4 < \varepsilon < 0.6$ is suitable to attenuate maximum wave energy and subsequently the wave force on the leeside wall can be reduced.
- The structural width is a key role phenomenon in the wave energy dissipation. In the case of the two porous blocks, the first structure shows relevant impact on the wave reflection and second structure is successful in regulating the wave transmission coefficient. However, the successful wave trapping is achieved in the confined region.
- In the presence of the leeward wall, the resonating peaks and troughs in the wave reflection and force can be reduced due to the construction of multiple porous blocks.

- The resonating peaks and troughs are useful in the design of coastal structures to find the optimum water chamber length and confined region spacing for the construction of the multiple porous blocks in the presence and absence of the leeward wall.
- The present method can be easily adopted in actual field for better wave blocking for the wave conditions within $0.5 < \gamma_{10}d < 1.0$ considering the medium porosity $\varepsilon = 0.4$ for better wave energy reflection and high porosity $\varepsilon = 0.8$ for better wave energy dissipation.

ACKNOWLEDGEMENTS

The authors are grateful to the Ministry of Human Resources Development (MHRD) Govt. of India and National Institute of Technology Karnataka Surathkal for providing necessary facilities for pursuing the research work.

REFERENCES

- Behera, H. and C. O. Ng (2018). Interaction between oblique waves and multiple bottom-standing flexible porous barriers near a rigid wall. *Meccanica* 53(4-5), 871-885.
- Belorgey, M., J. M., Rousset and G. Carpentier (2003). Perforated breakwaters, Dieppe harbour Jarlan Caisson: general schedule and acquired experience. *Proceedings of 13th International Offshore and Polar Engineering Conference. ISOPE, Honolulu, USA*, 850-857.
- Chwang, A. T. and A. T. Chan (1998). Interaction between porous media and wave motion. *Annual Review of Fluid Mechanics* 30(1), 53-84.
- Dalrymple, R. A., M. A. Losada and P. A. Martin (1991). Reflection and transmission from porous structures under oblique wave attack. *Journal of Fluid Mechanics* 224, 625-644.
- Das, P., D. P. Dolai and B. N. Mandal (1997). Oblique wave diffraction by parallel thin vertical barriers with gaps. *Journal of Waterway, Port, Coastal, and Ocean Engineering* 123(4), 163-171.
- Das, S. and S. N. Bora (2014). Reflection of oblique ocean water waves by a vertical rectangular porous structure placed on an elevated horizontal bottom. *Ocean Engineering*, 82, 135-143.
- Dattatri, J., H. Raman and N. J. Shankar (1978). Performance characteristics of submerged breakwaters. *In Coastal Engineering Proceedings*, 2153-2171.
- Hsu, H. H. and Y. C. Wu (1998). Scattering of water wave by a submerged horizontal plate and a submerged permeable breakwater. *Ocean Engineering* 26(4), 325-341.
- Huang, L. H. and H. I. Chao (1992). Reflection and

- transmission of water wave by porous breakwater. *Journal of Waterway, Port, Coastal, and Ocean Engineering*, 118(5), 437-452.
- Huang, Z., Y. Li and Y. Liu (2011). Hydraulic performance and wave loadings of perforated/slotted coastal structures: A review. *Ocean Engineering* 38(10), 1031-1053.
- Kaligatla, R. B., S. Tabssum and T. Sahoo (2018). Effect of bottom topography on wave scattering by multiple porous barriers. *Meccanica* 53(4-5), 887-903.
- Karmakar, D. and C. Guedes Soares (2015). Propagation of gravity waves past multiple bottom-standing barriers. *Journal of Offshore Mechanics and Arctic Engineering*, 137(1), 011101-10.
- Karmakar, D., J. Bhattacharjee and T. Sahoo (2010). Oblique flexural gravity-wave scattering due to changes in bottom topography. *Journal of Engineering Mathematics* 66(4), 325-341.
- Koley, S., A. Sarkar and T. Sahoo (2015a). Interaction of gravity waves with bottom-standing submerged structures having perforated outer-layer placed on a sloping bed. *Applied Ocean Research* 52, 245-260.
- Koley, S., H. Behera and T. Sahoo (2015b). Oblique wave trapping by porous structures near a wall. *Journal of Engineering Mechanics* 141(3), 04014122.
- Koraim, A. S., E. M. Heikal and O. S. Rageh (2011). Hydrodynamic characteristics of double permeable breakwater under regular waves. *Marine Structures* 24(4), 503-527.
- Laju, K., V. Sundar and R. Sundaravadivelu (2011). Hydrodynamic characteristics of pile supported skirt breakwater models. *Applied Ocean Research* 33(1), 12-22.
- Liu, Y. and H. J. Li (2013). Wave reflection and transmission by porous breakwaters: A new analytical solution. *Coastal Engineering* 78, 46-52.
- Losada, I. J., M. A. Losada and F. L. Martin (1995). Experimental study of wave-induced flow in a porous structure. *Coastal Engineering* 26(1-2), 77-98.
- Losada, I. J., M. D. Patterson and M. A. Losada (1997). Harmonic generation past a submerged porous step. *Coastal Engineering* 31(1-4), 281-304.
- Losada, I. J., R. Silva and M. A. Losada (1996). 3-D non-breaking regular wave interaction with submerged breakwaters. *Coastal Engineering* 28(1-4), 229-248.
- Madsen, O. S. and S. M. White (1976). Wave transmission through trapezoidal breakwaters. *Coastal Engineering Proceedings*, 2662-2676.
- Madsen, P. A. (1983). Wave reflection from a vertical permeable wave absorber. *Coastal Engineering* 7(4), 381-396.
- Mallayachari, V. and V. Sundar (1994). Reflection characteristics of permeable seawalls. *Coastal Engineering* 23(1-2), 135-150.
- Mendez, F. J. and I. J. Losada (2004). A perturbation method to solve dispersion equations for water waves over dissipative media. *Coastal Engineering* 51(1), 81-89.
- Neelamani, S., K. Al-Salem, and A. Taqi (2017). Experimental Investigation on Wave Reflection Characteristics of Slotted Vertical Barriers with an Impermeable Back Wall in Random Wave Fields. *Journal of Waterway, Port, Coastal, and Ocean Engineering* 143(4), 06017002-1-10.
- Newman, J. N. (1965a). Propagation of water waves past long two-dimensional obstacles. *Journal of Fluid Mechanics* 23(1), 23-29.
- Newman, J. N. (1965b). Propagation of water waves over an infinite step. *Journal of Fluid Mechanics* 23(2), 399-415.
- Newman, J. N. (1974). Interaction of water waves with two closely spaced vertical obstacles. *Journal of Fluid Mechanics* 66(1), 97-106.
- Rambabu, A. C. and J. S. Mani (2005). Numerical prediction of performance of submerged breakwaters. *Ocean Engineering* 32(10), 1235-1246.
- Reddy, M. G. and S. Neelamani (2006). Wave interaction with caisson defenced by an offshore low-crested breakwater. *Journal of Coastal Research*, 1767-1770.
- Sahoo, T., M. M., Lee and A. T. Chwang (2000). Trapping and generation of waves by vertical porous structures. *Journal of Engineering Mechanics* 126(10), 1074-1082.
- Sollitt, C. K. and R. H. Cross (1972). Wave transmission through permeable breakwaters. *Coastal Engineering Proceeding*, 1827-1846.
- Somervell, L. T., S. G. Thampi and A. P. Shashikala (2018). Estimation of friction coefficient for double walled permeable vertical breakwater. *Ocean Engineering* 156, 25-37.
- Sulisz, W. (1985). Wave reflection and transmission at permeable breakwaters of arbitrary cross-section. *Coastal Engineering* 9(4), 371-386.
- Ting, C. L., M. C. Lin and C. Y. Cheng (2004). Porosity effects on non-breaking surface waves over permeable submerged breakwaters. *Coastal Engineering* 50(4), 213-224.
- Twu, S. W. and C. C. Chieu (2000). A highly wave dissipation offshore breakwater. *Ocean Engineering* 27(3), 315-330.
- Twu, S. W. and D. T. Lin (1991). On a highly effective wave absorber. *Coastal Engineering* 15(4), 389-405.

- Wang, Y., G. Wang and G. Li (2006). Experimental study on the performance of the multiple-layer breakwater. *Ocean Engineering* 33(13), 1829-1839.
- Zhao, Y., H. J. Li and Y. Liu (2017). Oblique wave scattering by a submerged porous breakwater with a partially reflecting sidewall. *Journal of Marine Science and Technology* 25(4), 383-392.
- Zhao, Y., Y. Liu and H. Li (2016). Wave interaction with a partially reflecting vertical wall protected by a submerged porous bar. *Journal of Ocean University of China* 15(4), 619-626.
- Zhu, S. (2001). Water waves within a porous medium on an undulating bed. *Coastal Engineering* 42(1), 87-101.
- Zhu, S. and A. T. Chwang (2001). Analytical study of porous wave absorber. *Journal of Engineering Mechanics* 127(4), 326-332.